



Allele-tagged TaqMan® PCR genotyping assays for high-throughput detection of soybean cyst nematode resistance

Mariola Usovsky¹ · Kristin Bilyeu² · Andrew Bent³ · Andrew M. Scaboo¹

Received: 19 September 2024 / Accepted: 15 November 2024
© The Author(s) 2024

Abstract

Background Whole genome resequencing (WGRS) platforms provide exceptional fingerprinting of the entire genome but are expensive and less flexible to use as a routine genotyping tool for targeting causal polymorphisms within a germplasm collection or breeding program. Therefore, there has been a continuous effort to develop small-scale genotyping platforms that facilitate robust and quick assessments of the allelic status of causal variants for important traits within soybean breeding programs. The objective was to develop a comprehensive panel of soybean cyst nematode (SCN) resistance TaqMan® assays via selecting the causative genes and analyzing their associated alleles.

Methods The Soybean Allele Catalog was utilized to investigate WGRS-derived variants which are predicted to cause a change in the amino acid sequence of a gene product. This panel of TaqMan® assays reflects current knowledge about known SCN resistance-causing genes and their associated alleles: *GmSNAP18-a* and *-b*, *GmSNAP11*, *GmSHMT08*, *GmSNAP15*, *GmNSF_{RAN07}*, and *GmSNAP02-ins* and *-del*. Developed assays were tested using elite breeding lines and segregating populations. TaqMan assays were compared to other currently available KASP and CAPS assays.

Conclusion All assays showed excellent allele determination efficiencies. This SCN genotyping assay panel can be utilized as a simplified, accurate and reliable genotyping platform further equipping the updated soybean breeding toolbox.

Keywords TaqMan · Soybean cyst nematode · Molecular markers · Soybean · Disease resistance · Genotyping

Introduction

Plant breeding is one of the applied research areas that has benefited from the current advances in molecular marker technologies [1]. Genome-scale next generation sequencing technologies enable fingerprinting of millions of single nucleotide polymorphisms (SNPs) and insertion/deletion mutations (InDels) that can be utilized in identification of quantitative trait loci (QTL) and genes governing traits of interest [2, 3]. However, genome-scale sequencing platforms are expensive and less flexible to use as a routine genotyping

tool for targeted traits. As a result, there has been a continuous effort to develop small-scale lower-density genotyping platforms that facilitate robust and cost-effective assessment of breeding material [4, 5]. Variant and causal polymorphisms associated with desirable plant traits are commonly used as molecular markers in breeding programs via marker-assisted selection (MAS). Molecular markers are a useful tool for selecting genomic regions correlated with key qualitative and quantitative traits, especially when the costs of phenotyping greatly exceed the costs of genotyping, and when newer methods including genomic selection have low prediction accuracies. SNP markers are preferred among breeders and molecular biologists because of their low cost, high genomic abundance, locus specificity, co-dominant inheritance, amenability to high-throughput genotyping, and low genotyping error rates [1]. Multiple chemistries and assays have been developed for SNP genotyping including mass spectrometry, oligonucleotide arrays, single stranded conformational polymorphism, and sequencing. Some of the most widely used technologies tend to be centered on a fluorescence-based polymerase chain reaction

✉ Mariola Usovsky
mariolausovsky@missouri.edu

¹ Division of Plant Science and Technology, University of Missouri, Columbia, MO 65211, USA

² Plant Genetics Research Unit, United States Department of Agriculture-Agricultural Research Service, University of Missouri, Columbia, MO 65211, USA

³ Department of Plant Pathology, University of Wisconsin, Madison, WI 53706, USA

(PCR) assay i.e. 5' nuclease, Molecular Beacon, Scorpion™, KASP™, TaqMan®, PACE®, Amplifluor®, and Invader® [2, 6–8]. With all these methods, the allele-specific discrimination ability is solely based on either probe hybridization or primer extension.

TaqMan® (Applied Biosystems, Foster City, CA) is a genotyping system that is in high demand due to its large-scale high-throughput application [3, 9]. TaqMan® chemistry is widely used to reliably genotype multiple allele-specific polymorphic variant types in a genome including SNPs, small Indels, and presence/absence variants [6]. It requires a low amount of template DNA, and its allele cluster separation is clear. In the classical definition of TaqMan® genotyping, the allelic specificity is provided by two probes labelled with distinct fluorescent reporter dyes. With fluorophore detection, probes are made of a fluorescence resonance energy transfer (FRET) cassette, which is labeled with a fluorescent reporter dye fused to the 5' end of probe, and the non-fluorescent quencher (NFQ) attached to the 3' end [9]. The minor groove binder (MGB) technology enables TaqMan® probes to increase specificity and sensitivity for superior discrimination of highly homologous allele sequences via increasing the melting temperature (T_m) of the probe and stabilizing probe–template hybrids. During the PCR process, the generic primers allow the amplification of the short sequence for the probes to detect their complementary sequence. The alleles are detected by the corresponding fluorescence signal generated via 5' exonuclease cleavage of the FRET cassette that liberates the reporter dye from the quencher, resulting in fluorescence signal. If both fluorescent signals were produced at the same time, it would suggest that the sample was a heterozygote.

TaqMan® genotyping is used in soybean breeding for trait improvement via marker-assisted selection (MAS) [8, 10, 11]. Soybean cyst nematode (SCN; *Heterodera glycines*) is the number one pest of soybean and is primarily managed through resistant cultivars [12, 13]. In recent years, significant progress has been made to discover genes that control SCN resistance [14]. Several *Rhg* (for resistance to *H. glycines*) genes have been shown to play a role in SCN resistance including the two *GmSNAP18* alleles: *GmSNAP18-a* (encoded within the multicopy four-gene *rhg1-a* haplotype) and *GmSNAP18-b* (encoded within the multicopy four-gene *rhg1-b* haplotype) at the *Rhg1* locus [15, 16], *GmSNAP11* at the *Rhg2* locus [17–21], *GmSHMT08* at the *Rhg4* locus [22], *GmNSF_{RAN07}* [18], *GmSNAP15* (also known as *cqSCN-006*) [23], and two alleles of *GmSNAP02* [24]. The *GmSNAP18*, *GmSNAP11*, and *GmSNAP02* genes encode α -soluble NSF (*N*-ethylmaleimide-sensitive factor) attachment proteins known as α -SNAPs, *GmSNAP15* gene encodes γ -soluble NSF attachment protein known as γ -SNAP, *GmSHMT08* gene encodes the enzyme serine hydroxyl methyltransferase, and *GmNSF_{RAN07}* encodes an atypical form of

N-ethylmaleimide sensitive factor or NSF protein [16, 18, 21–24].

Although several assays have been developed for detection of a few SCN resistance genes, most of them are based on another leading SNP genotyping technology known as Kompetitive allele-specific PCR (KASP). In contrast to TaqMan®, the allelic specificity of KASP genotyping platform is provided by two forward primers with the target SNP positioned at their 3'-end, and fluorescence-labelled reporter dyes at 5'-end, while one common generic reverse primer is designed using the targeted genomic sequence [7, 25].

The Soybean Allele Catalog (SAC) is a web tool which can be queried to obtain the series of alleles present in a gene of interest, based on the set of gene-modifying variants present in a diversity panel of 1,066 wild and domesticated soybean accessions [26]. The gene-modifying variants are whole genome resequencing (WGRS)—derived variants predicted to cause a change in the amino acid sequence of a gene product. This study was conducted to develop a comprehensive panel of TaqMan® assays that can be used for MAS breeding. Alleles of each gene have been analyzed using the SAC and raw sequencing reads, and selected variants were targeted to develop functional markers that had the highest likelihood of association between genotype and known phenotype. Performance of the assays has been evaluated in term of design flexibility, allele calling and allele discriminating efficiency and accuracy.

Materials and methods

Plant materials and DNA extractions

Three sets of plant material were used in this study: (Set 1) 51 plant introductions (PIs) whole genome re-sequenced (WGRS) as a part of the Soy1066 WGRS set with known phenotypes [27] to select the correct allele and validate the accuracy of each assay; (Set 2) 619 elite breeding lines from the northern soybean breeding program at the University of Missouri to test assay performance and assess the frequency of selected alleles; and (Set 3) multiple segregating breeding populations from the northern soybean breeding program at the University of Missouri to determine the placement of heterozygotes on the discrimination plot. For Set 1, PIs were requested from the United States Department of Agriculture—Agricultural Research Service (USDA-ARS) Germplasm Resources Information Network (GRIN), and young trifoliate leaf tissue was collected from bulking tissue from six plants. For Sets 2 and 3 young trifoliate leaf tissue was collected from single plants.

Total genomic DNA was extracted using a non-hazardous sodium dodecyl sulfate (SDS) method [28] with minor modifications. Young leaves were placed into 1.1 mL tissue

collection tubes (National Scientific) and positioned on matrix latch racks (Thermo Scientific) with its corresponding sample number. One 4 mm O.D. glass bead (Chemglass Life Sciences) was added to each tube, and racks were sealed with silicone plate mats (Thermo Scientific) and stored in -80°C . Frozen racks were then placed in a Mini-BeadBeater (Biospec Products) for 30 s at 2200 rpm to grind tissue. Six hundred microliter of the combined NaCl and extraction buffer [40% (v/v) 5 M NaCl and 60% (v/v) extraction buffer (0.5% SDS, 200 mM Tris-Cl pH 7.5, 250 mM NaCl, 25 mM EDTA,)] was added to each well and mixed in a Mini-BeadBeater for 30 s at 2200 rpm. The samples were then left in a dry air incubator at 65°C . After 1 h, plates were shaken manually for a few seconds and centrifuged for 15 min at 4700 G. Two hundred microliter of supernatant was transferred to 96 well 2 mL-deep plates (Thermo Scientific) containing 200 μL ice cold ethanol, sealed with silicone mats (Axygen), and inverted several times to precipitate DNA. The plates were then centrifuged for 10 min at 4700 G. Ethanol was removed by inverting the plates upside down and placing them on a tissue paper to remove excess liquid. Pellets were left to air dry overnight. The next day, 200 μL of double distilled water was added to each sample to resuspend the pellets and plates were stored at -20°C . DNA concentrations were quantified using NanoDrop One (Thermo Scientific) and normalized to 50 ng/ μL using Mantis® automated liquid handler (Formulatrix).

Variant Allele Identification

The Soybean Allele Catalog (SAC) was utilized to analyze WGRS-derived variants among 1,066 (Soy1066 WGRS set) soybean accessions ([26]). A variant was defined as a single physical position which is predicted to cause a change in the amino acid sequence of a gene product. All variant positions were reported based on the Wm82.a2.v1 reference genome. An allele was defined as a unique variant or set of variants within the target gene. Alleles were selected based on known phenotypic reactions of the soybean resistant and susceptible lines [27]. Analyzed genes were *GmSNAP18* (*Glyma.18G022500*), *GmSNAP11* (*Glyma.11G234500*), *GmSHMT08* (*Glyma.08G108900*), *GmNSF07* (*Glyma.07g195900*), *GmSNAP15* (*Glyma.15G191200*), and *GmSNAP02* (*Glyma.02G260400*). The genes' structure was compared on Phytozome to confirm their variants (<https://phytozome-next.jgi.doe.gov>). The target allele was assigned as mutant (MUT) at one specific variant position, whereas the other remaining alleles were marked as wild type (WT). Frequencies of MUT alleles in the Soy1066 WGRS set were calculated based on the percentage of lines with MUT allele versus a total number of 1,066 soybean lines (100%). Frequencies of MUT alleles in the elite breeding lines set were calculated based on the percentage of lines with MUT allele

detected at a selected variant position versus a total number of genotyped lines (100%). The assays were named to signify target MUT allele that indicates resistance: MU-SNAP18-A detects *GmSNAP18-a*, MU-SNAP18-B detects *GmSNAP18-b*, MU-SNAP11-SP detects *GmSNAP11-Sp*, MU-SHMT08 detects *GmSHMT08-R*, MU-SNAP15 detects *GmSNAP15-R*, and MU-NSF-RAN07 detects *GmNSF_{RAN07}*. Assay MU-SNAP18-C was developed to separate *GmSNAP18-a* and *GmSNAP18-b* from additional alleles of *GmSNAP18*. Assays MU-SNAP02^{INS}-WT, MU-SNAP02^{INS}-MUT, MU-SNAP02^{DEL}-1, and MU-SNAP02^{DEL}-2 [24] were used for validation and genotyping comparisons (Supplementary Table 1).

Based on the SAC, *GmSNAP18* gene carries seven gene-modifying variants creating five alleles. The *GmSNAP18-a* allele, present in many SCN resistant lines including Peking, PI 90763, and PI 437654, has a missense variant at the physical position Gm18:1,643,660 (Wm82.a2.v1). The other four alleles displayed the same sequence as in the reference genome Williams 82 (*GmSNAP18-Ref*) at this variant position, including *GmSNAP18-b*. In the *GmSNAP18-a* allele, Williams 82 has a "C" nucleotide, whereas Peking has "G" nucleotide (GID208E), and therefore the aspartic acid (D) is replaced by glutamic acid (E). Both amino acids are acidic with negative charges and carboxyl groups. MU-SNAP18-A assay was designed for detection of missense mutation GID208E (Supplementary Fig. 1).

The *GmSNAP18-b* allele, present in PI 88788 and PI 209332, has three unique missense mutations in the *GmSNAP18* gene based on SAC. The first variant (AIQ203K) replaces the "C" nucleotide of Williams 82 with the "A" nucleotide in PI 88788 at the physical position Gm18:1,643,643. This change causes a replacement of glutamine (Q), a hydrophilic uncharged amino acid with an amide group, to lysine (K), a basic positively charged amino acid with an amine group. The second variant (CIE285Q) replaces the "G" nucleotide of Williams 82 with the "C" nucleotide in PI 88788 at the physical position Gm18:1,645,400 and causes an exchange of basic negatively charged glutamic acid (E) to a polar uncharged glutamine (Q). The third variant (CID286H) replaces the "G" nucleotide of Williams 82 with the "C" nucleotide in PI 88788 at the physical position Gm18:1,645,403 causes a replacement of negatively charged aspartic acid (D) to positively charged histidine (H). These missense variants have been described in previous studies [15, 27]. MU-SNAP18-B assay was designed for detection of missense mutation AIQ203K (Supplementary Fig. 2).

MU-SNAP18-C assay (Fig. 3; Supplementary Fig. 3) was developed to separate two resistant alleles, *rhg1-a* and *rhg1-b*, from susceptible alleles (*GmSNAP18-Ref*, *Rhg1-c*). This assay targets the position Gm18:1,645,409 of the *GmSNAP18* gene where a missense mutation (AIL288I) replaces the "C" nucleotide of Williams 82 with the "A"

nucleotide in PI 88788 (*rhg1-b*) and Peking (*rhg1-a*). This causes a substitution of a hydrophobic alanine (A) with a hydrophobic isoleucine (I). Due to other polymorphisms found nearby the target position, the probe detecting the *Rhg1-c* allele anneals to three polymorphisms: G1Ref (Gm18:1,645,403), A1Ref (Gm18:1,645,407) and C1Ref (Gm18:1,645,409). Besides the target polymorphism AIL288I (Gm18:1,645,409) that is the same for *rhg1-a* and *rhg1-b* alleles, the second probe anneals to an additional variant that causes a disruptive in-frame insertion. This three-nucleotide insertion, at the position Gm18:1,645,407, is slightly different in *rhg1-a* (AGGTID287delinsEV) and *rhg1-b* (AGGCID287delinsEA) alleles. The second probe was designed to anneal to two variants within the *rhg1-b* allele; however, the probe was able to align with the *rhg1-a* allele where the mismatch exists at the 3' end of the probe. This allowed a separation of the *rhg1-b* and *rhg1-a* alleles into two separate MUT1 and MUT2 clusters, respectively.

The SAC revealed eight gene-modifying variants on the coding sequence of the *GmSNAP11* gene. Among nine alleles, *GmSNAP11-Sp* was selected as a resistance-causing allele. It has a splice and intron variant (Alintron_variant & splice_donor_variant) at the physical position Gm11:32,969,916 that is caused by a substitution of the single nucleotide “C” in Williams 82 to the “A” present in genotypes such as Peking, PI 437654, and PI 88788. MU-SNAP11-SP assay was designed to target this mutation (Supplementary Fig. 4). The splice site SNP causes an amino acid frameshift and premature termination after A239 in *GmSNAP11-Sp*, when compared with full sequence of 289 amino acids in Williams 82 [18, 21, 29–31]. The *GmSNAP11-Sp* mutant mis-spliced RNA continues with the intron sequence that gets translated into three new amino acids before a stop codon. This intron retention (IR) is a well-conserved form of alternative splicing. A widely accepted function of IR is to regulate gene expression via nonsense-mediated decay (NMD), triggered by intronic premature termination codons (PTCs), or IR transcript retention and degradation in the nucleus [32].

There were 14 gene-modifying variants in the coding sequence of the *GmSHMT08* gene that resulted in 13 alleles. The *GmSHMT08-R* resistant allele has two unique missense variants GIP200R and TIN428Y at the physical positions: Gm08:8,361,148 and Gm08:8,361,924, respectively. In comparison with SAC, Phytozome Wm82.a2 displayed an extra 70 amino acids at the beginning of the protein. Due to an automated annotation error in *Glyma.08G108900* in Phytozome, all variants are shifted, and therefore GIP200R and TIN428Y in SAC correspond to GIP130R and TIN358Y in Phytozome. The variant GIP130R, is caused by SNP of “C” nucleotide in Williams 82 to “G” nucleotide that causes change of proline (P), a hydrophilic polar uncharged aromatic amino acid, to arginine (R), a basic positively

charged amino acid with an amine group. The second variant TIN313Y&N358Y&N389Y is caused by SNP of “A” nucleotide in Williams 82 to “T” nucleotide that replaces a hydrophilic polar uncharged amide group asparagine (N) to a hydrophilic polar uncharged phenyl group tyrosine (Y). This double variant allele showed impairment of folate binding affinity and reduced tetrahydrofolate (THF)-dependent enzyme activity in the SCN-resistant soybean cultivar (cv.) Forrest [33]. Recently, individual effects of the P130R and N358Y single variants were analyzed on the enzyme function and concluded that both variants have reduced THF-dependent catalytic activity [34]. The resistant allele of P130R/N358Y double variant in Forrest produces unique and unexpected effects on the SHMT08 enzyme, which cannot be easily predicted using individual variants. No single variant allele was present in the SAC sequencing set, therefore the MU-SHMT08 assay was designed to target P130R variant (Supplementary Fig. 5).

GmSNAP15, at the *cqSCN-006* locus, encodes a gamma SNAP (γ -soluble NSF attachment protein) [23]. The SAC revealed seven missense variants in the *GmSNAP15* gene that caused eight alleles. *Glycine soja* PI 468916, which carries the resistant form of the gene, did not show a difference in the predicted protein product in comparison with the reference genome Williams 82. De novo WGS assembly of PI 468916 along with cloned fosmids, from a fosmid library generated from PI 468916, were used to identify structural variations of the gene in comparison with Williams 82 [23]. There were numerous DNA polymorphisms in the inferred regulatory region of the promoter and gene body; however, only one synonymous mutation at the position Gm15:20,631,002 within the 5th exon was present between PI 468916 (and the resistant line LD10-30110 derived from PI 468916) and Williams 82 sequences. Therefore, this silent mutation was utilized to develop the assay MU-SNAP15 (Supplementary Fig. 6). The “G” nucleotide in Williams 82 was replaced with “T” nucleotide in PI 468916.

GmNSF07 (*Rhg1*-associated NSF on chromosome 07) and *GmSNAP18* promote cellular vesicular trafficking by mediating the disassembly and reuse of soluble NSF attachment protein receptor (SNARE) protein complexes [35]. An atypical form of NSF protein contains unique N-domain polymorphisms that mitigate the cytotoxicity and cause improved affinity in binding the SCN resistance-conferring *Rhg1* α -SNAPs [18]. Soybeans that carry *rhg1-a* or *rhg1-b* alleles are not viable if they do not also carry *GmNSF_{RAN07}*, a fact that can cause linkage distortion and unexpected gene segregation ratios during breeding for the respective chromosome 18 and chromosome 07 genetic intervals. The *GmNSF07* gene has 11 gene-modifying variants in the coding sequence creating nine alleles. The *GmNSF_{RAN07}* allele present in SCN-resistant lines has a conservative in-frame insertion of three nucleotides in position Gm07:36,448,342

(Wm82.a2.v1) that causes a duplication of phenylalanine (F), a basic positive charge amino acid with amine group (CAAAlconservative_inframe_insertion|F115dup). This in-frame insertion variant was selected as a likely causative mutation due to its presence at the predicted α -SNAP/NSF interface and its presence in multiple SCN resistant lines including PI 88788, Peking, PI 90763, and PI 437654. This CAAAlconservative_inframe_insertion|F115dup variant was used to design MU-NSF-RAN07 assay (Supplementary Fig. 7). Four alleles of the *GmNSF07* gene have this insertion variant, however, some of these alleles were present in only one or two soybean genotypes. Therefore, the *GmNSF_{RAN07}* allele was designated to Forrest as the *GmNSF_{RAN07}* was discovered in this cultivar [18]. The selected allele has other four missense variants at the positions Gm07:36,447,402 (AlM180I), Gm07:36,448,951 (TIS25N), Gm07:36,448,964 (AlN21Y), and Gm07:36,449,014 (TIR4Q).

It was recently discovered that the *GmSNAP02* gene (*Glyma.02G260400*) plays a role in SCN resistance through its loss of function caused by two alleles: *GmSNAP02-ins* and *GmSNAP02-del* [24]. The *GmSNAP02-ins* allele is caused by an ~6 kb insertion in the eighth exon in PI 90763. This variant is not reflected in the SAC, but it is indicated by imputation when extracting the raw data from SAC. The *GmSNAP02-del* allele is caused by a 22-nucleotide deletion in the first exon at the physical position Gm02:44,695,753 (Wm82.a2.v1) in PI 437654 [24]. Based on SAC, there are three distinct nucleotide changes at this variant position. The first one is the "C" nucleotide present in ten alleles of *GmSNAP02*. It is present in genotypes such as the reference genome Williams 82, Peking, and PI 90763, and named as *GmSNAP02-Ref* allele. The second has a missense mutation where the "C" nucleotide is replaced with "G" alternative nucleotide in genotypes such as Forrest, PI 88788, and PI 209332, and therefore named as *GmSNAP02-Alt* allele. The third one displays a 22-nucleotide deletion *GmSNAP02-del* allele in PI 437654, Hartwig and PI 89772 (Clframeshift_variant|A8fs). Assays MU-SNAP02^{INS}-WT, MU-SNAP02^{INS}-MUT, MU-SNAP02^{DEL}-1, and MU-SNAP02^{DEL}-2 have been previously described [24] and were tested using sample Sets 1 through 3.

TaqMan[®] genotyping assays

The assays were manufactured by ThermoFisher Scientific through Custom TaqMan[®] Assay Design Tool (<https://www.thermofisher.com/order/custom-genomic-products/tools/genotyping>) by entering DNA sequence or designed primer and probe pair sequences selected via PrimerQuest[™] Tool (Integrated DNA Technologies) (Table 1; Supplementary Table 1). PCR reactions were carried out in total volumes of 4 μ L containing 1X TaqMan[®] Universal PCR Master Mix II (Thermo Fisher Scientific), 5 \times TaqMan[®] Genotyping

Assay, and 100 ng genomic DNA. Thermal cycling profiles were based on the manufacturer recommended protocol. The reactions were run on a LightCycler[®] 480 (Roche Diagnostics) instrument with the following thermal cycling profile: (1) denaturation at 95 $^{\circ}$ C for 10 min; (2) ten cycles of touch down of 92 $^{\circ}$ C for 15 s and 68–60 $^{\circ}$ C (0.8 $^{\circ}$ C drop in each cycle for 1 min; (3) 30 cycles of amplification at 92 $^{\circ}$ C for 15 s and 60 $^{\circ}$ C for 1 min; and (4) final plate read at 60 $^{\circ}$ C. Allelic discrimination analysis was performed on a LightCycler[®] 480 software with the end-point genotyping algorithm function and two opposite homozygous genotypes were plotted into two clusters near two axes and the heterozygous genotypes were clustered between the two clusters for homozygous genotypes. The homozygous alleles labelled with VIC[®] dye were grouped into the allele Y (green cluster), while homozygous alleles labelled with FAM[®] dye were grouped into the allele X (blue cluster). Mutant cluster (MUT) was designated as a desirable SCN resistance-causing allele, whereas wild type cluster (WT) was designated as other alleles described by a specific variant position where the assays have been designed. In addition to test samples, four control samples were included on each plate to confirm the allelic status of each cluster.

TaqMan[®] assay is based on DNA amplification in the presence of two allele-specific probes that emit fluorescence at different wavelengths (TaqMan[®] SNP Genotyping Assays User Guide 2017, Thermo Fisher Scientific Inc.). In this research, TaqMan[®] MGB probes were labelled with fluorescent reporter dyes FAM[®] and VIC[®] linked to the 5' end of the probe, and NFQ at the 3' end. This technology increases the stability and specificity of probe hybridization and enhances spectral performance (TaqMan[®] SNP Genotyping Assays User Guide 2017, Thermo Fisher Scientific Inc.). During PCR, the annealed TaqMan[®] probe is degraded by the *Taq* polymerase, and the fluorescence signal is generated by free reporter through FRET. Using coordinate geometry principles, six assessments were done to determine allelic discrimination of each assay. Samples that fail the amplification and NTC should not emit a fluorescence signal and therefore their position on the plot should be at 0/0 (axis x/y). In an ideal case scenario of an allele discrimination plot, homozygous cluster of allele X lies along the horizontal axis producing high FAM[®] and low VIC[®] signal, while homozygous cluster of allele Y is expected to be parallel with the vertical axis y producing high VIC[®] and low FAM[®] signal. Heterozygotes are shown using segregating populations and were expected to cluster along the diagonal line with nearly equal FAM[®] and VIC[®] signals. Cluster to axis separation angles were used to determine the discrimination efficiency of homozygous clusters. The smaller the size of angle between axis and its corresponding allele cluster, the higher the discrimination efficiency. Homozygous cluster to heterozygous cluster separation angles were used to

determine HET genotypes. Barring investigator error, allele call rate and assay accuracy should be 100%.

Plot evaluation metrics

Six metrics were utilized to evaluate allelic discrimination on the end-point genotyping clustering plots [25, 36]:

- (1) The coordinates of the no template control (NTC). The NTC samples should not emit fluorescence signal and therefore its position should be at the bottom left corner at position 0/0 (x/y axis). Location of NTC is the mean of FAM[®] and VIC[®] fluorescence signal of NTC reactions. No amplification samples should cluster with NTC.
- (2) Homozygous cluster to axis separation angle: Cluster X to axis X separation angle described as an angle size between the horizontal X-axis and the line connecting a cluster generated from the high FAM signal (allele X) with the NTC coordinate; Cluster Y to axis Y separation angle described as an angle size between the horizontal Y-axis and the line connecting a cluster generated from the high VIC signal (allele Y) with the NTC coordinate.
- (3) Homozygous cluster to heterozygous (HET) cluster separation angle: Cluster X to cluster HET separation angle described as an angle size of the homozygous cluster X to HET cluster; Cluster Y to cluster HET separation angle described as an angle size of the homozygous cluster Y to HET cluster.
- (4) Cluster to NTC distance and Cluster Spread determine possibility of trailing clusters usually caused by unequal quantity of DNA or pipetting errors.
- (5) Allele call rate: determined based on Set 1 as the percentage of successful genotype calls via sample amplification. No amplification was considered as unsuccessful genotype call.
- (6) Assay accuracy was measured based on Set 1 as matching a detected allele with a variant from WGRS.

Results

Detection of *GmSNAP18-a* and *GmSNAP18-b* resistance alleles

Among the four genes tandemly repeated at the *Rhg1* locus, only *GmSNAP18* (*Glyma.18G022500*) displayed polymorphisms based on the Soybean Allele Catalog. The *GmSNAP18* gene has two known SCN resistance alleles: *GmSNAP18-a* (within *rhg1-a*, for example in Peking) and *GmSNAP18-b* (within *rhg1-b*, for example in PI 88788). Those alleles encode the proteins α -SNAP_{Rhg1}LC and

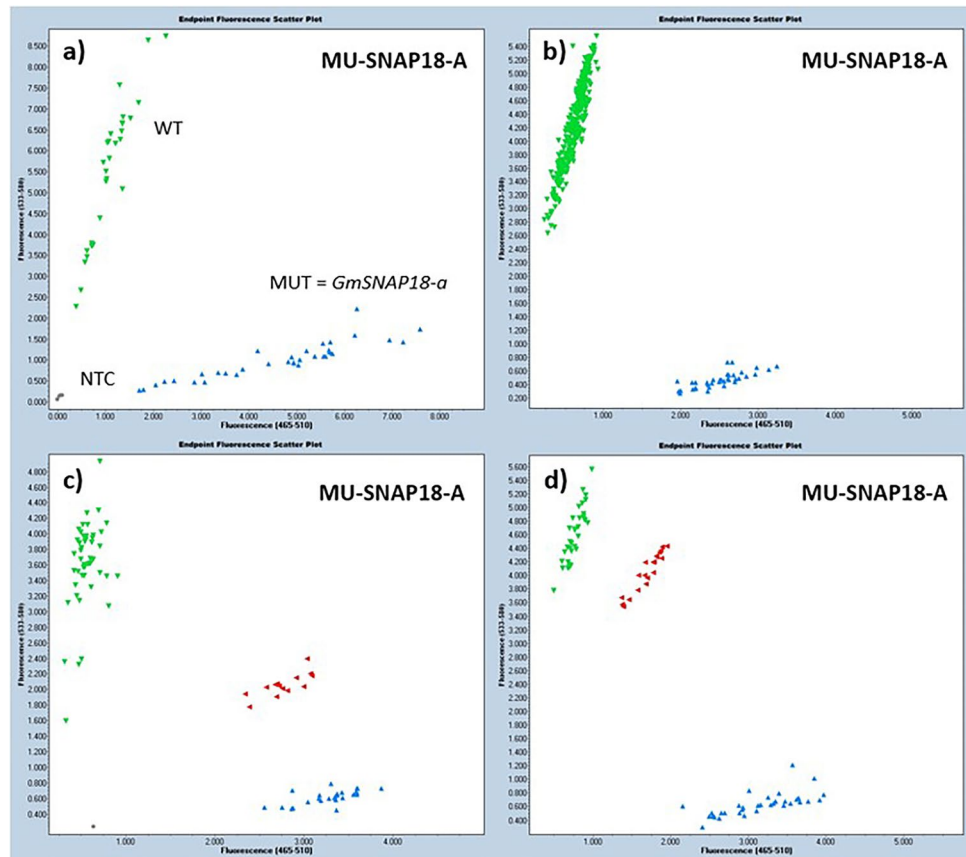
α -SNAP_{Rhg1}HC respectively [18]. All studied multicopy *rhg1-b* haplotypes also carry one copy of the *GmSNAP18-c* allele, which encodes a Williams 82-type α -SNAP_{Rhg1} WT protein that carries a C-terminus more similar to most other plant and animal α -SNAP proteins [30, 37]. To determine which allele is present in each soybean genotype and to separate from other alleles including *GmSNAP18-Ref* in Williams 82, three assays were developed: MU-SNAP18-A, MU-SNAP18-B, and MU-SNAP18-C to detect *GmSNAP18-a*, *GmSNAP18-b*, and both alleles, respectively.

MU-SNAP18-A assay (Fig. 1; Supplementary Fig. 1) was developed to separate the FAM[®]-labelled *GmSNAP18-a* resistance allele (MUT cluster) from the other VIC[®]-labelled alleles of *GmSNAP18* (WT cluster). Discrimination clustering plots displayed discernable separation between homozygous clusters with a small separation angle to the X and Y axis. The clusters were tight, and the NTC did not show a fluorescence signal. Heterozygotes were tested on two populations that segregate for *rhg1-a* and *Rhg1-c* (Fig. 1c) as well as *rhg1-a* and *rhg1-b* (Fig. 1d), and the HET cluster was slightly skewed to the MUT and WT cluster, respectively. In both populations, the heterozygotes produced the intermediate cluster. The allele call rate and assay accuracy were 100% (Fig. 1a, Supplementary Table 2). The *GmSNAP18-a* allele was present in 49 accessions (4.6%) in the Soy1066 WGRS set, and 59 elite breeding lines (9.5%) within the breeding program (Fig. 1b).

MU-SNAP18-B assay (Fig. 2; Supplementary Fig. 2) was developed to target a missense mutation AIQ203K, and it separates the FAM[®]-labelled *GmSNAP18-b* resistance allele (MUT cluster) from the VIC[®]-labelled alleles of *GmSNAP18* (WT cluster). While the WT cluster positioned along the Y axis, wide distribution of samples within the Y cluster was present. The MUT cluster was skewed away from X axis and the HET cluster was not easily detectable (Fig. 2a, b). Analyzing a population that segregates for *Rhg1-c* and *rhg1-b* with Rhg1-2 [38] and SNAP18-1 [39] KASP assays, and a population that segregates for *rhg1-a* and *rhg1-b* with MU-SNAP18-A assay, determined the location of HETs that clustered directly above the MUT cluster in the discrimination plot produced by the MU-SNAP18-B assay (Fig. 1c, d). The NTC did not emit fluorescence, and the allele call rate and assay accuracy were 100% (Supplementary Table 2). The assay accuracy was 98% due to discrepancies in allele call of PI 567416 that was located in MUT cluster rather than WT. The *GmSNAP18-b* allele was present in 50 accessions (4.7%) of the Soy1066 WGRS set, and 409 breeding elite lines (66%).

The MU-SNAP18-C (Fig. 3; Supplementary Fig. 3) assay was developed to separate two resistant alleles, *rhg1-a* and *rhg1-b*, from susceptible alleles. Two MUT clusters, MUT1 and MUT2, corresponded to detection of *GmSNAP18-b* and *GmSNAP18-a*, respectively. The MUT1 cluster showed a

Fig. 1 Discrimination clustering plots of samples genotyped with MU-SNAP18-A assay for detection of the *GmSNAP18-a* (*rhg1-a*) allele: **a** a set of whole genome re-sequenced GRIN lines; **b** elite breeding lines, and **c, d** F₃ populations of either **c** SA18-13420×U15-322140 that segregates for *rhg1-a/Rhg1-c*, or **d** JTN-5516×LD11-2170 that segregates for *rhg1-a/rhg1-b*. The fluorescence of FAM on X-axis was designed to detect the homozygous resistance mutant (MUT) allele (blue). The fluorescence of VIC on Y-axis detects a combination of susceptible wild type (WT) alleles and homozygous resistance alleles that are not desirable (green). Heterozygotes were clustered within the intermediate (red). NTC = no template control (grey)



stronger signal than MUT2 cluster, however, most samples were skewed away from the X axis (Fig. 3a, b). In the *rhg1-b/Rhg1-c* segregating population, although MUT1 and HET clustered close to each other, MU-SNAP18-C assay (Fig. 3c) improved the selection of heterozygotes when compared to MU-SNAP18-B assay (Fig. 2c). In the *rhg1-a/Rhg1-c* segregating population, the clustering plot (Fig. 3d) was comparable to the plots created by MU-SNAP18-A (Fig. 1c). For this assay, PI 567416 was also located in the MUT1 cluster, therefore, the assay accuracy was 98%.

Detection of *GmSNAP11-Sp* resistance allele at the *Rhg2* locus

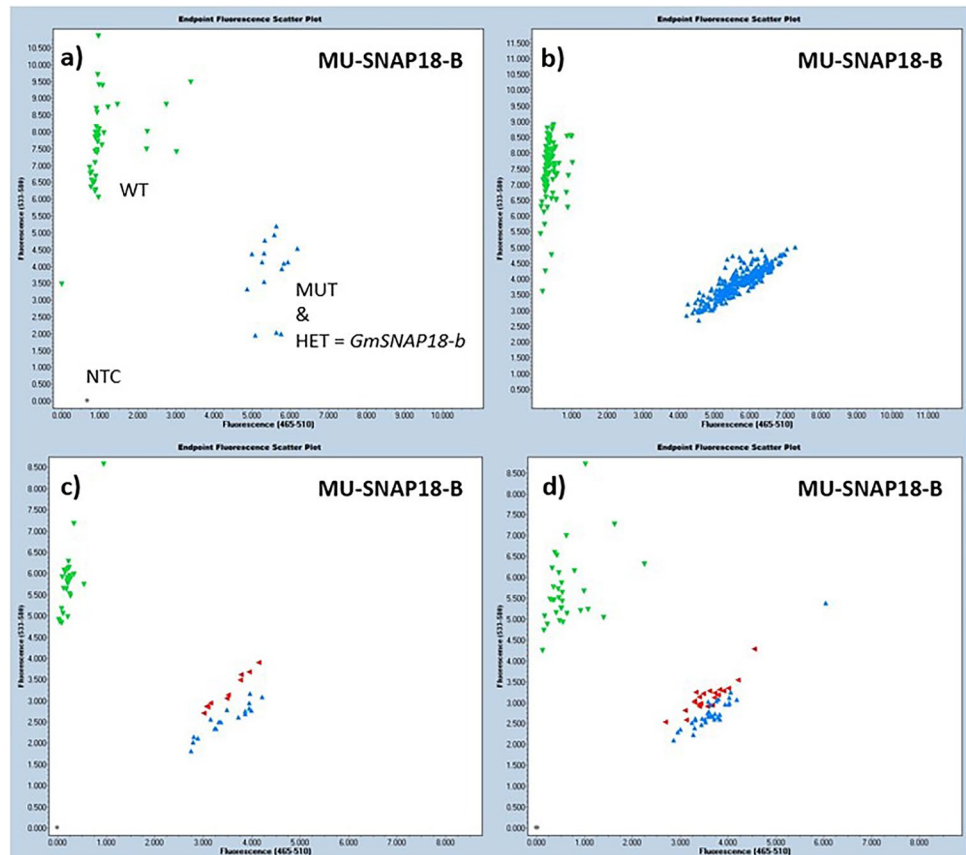
MU-SNAP11-SP assay was designed to detect a splicing variant. The *GmSNAP11-Sp* allele was present in 108 accessions (10.1%) of the Soy1066 WGRS set, and 229 breeding elite lines (37%). MU-SNAP11-SP assay (Fig. 4; Supplementary Fig. 4) separates the VIC[®]-labelled *GmSNAP11-Sp* resistance allele (MUT cluster) from FAM[®]-labelled other eight alleles of *GmSNAP11* (WT cluster). The discrimination plots displayed MUT cluster along the Y axis, however the WT cluster was skewed towards the heterozygotes (Fig. 4a, b). The HET cluster was distinguishable from the WT cluster in a segregating

population (Fig. 4c). The no-template control did not show any fluorescence signal. The allele call rate and assay accuracy were 100% (Fig. 4a; Supplementary Table 3).

Detection of *GmSHMT08-R* resistance allele at the *Rhg4* locus

MU-SHMT08 assay (Fig. 5; Supplementary Fig. 5) was designed to target the missense variant GIP130R and it separates the FAM[®]-labelled *GmSHMT08-R* resistance allele (MUT cluster) from the other VIC[®]-labelled alleles (WT cluster). While the WT cluster produced a strong fluorescent signal and was situated along the Y axis, the MUT cluster was slightly skewed away from the X axis (Fig. 5a, b). Moreover, although the MUT cluster was compacted, it was at a close distance to the NTC. However, the clustering was well defined between homozygous and heterozygous clusters in a segregating population (Fig. 5c). The HET cluster was slightly skewed towards the WT cluster. The NTC did not generate any fluorescence. The allele call rate and assay accuracy were 100% (Supplementary Table 3). The *GmSHMT08-R* allele was present in 40 accessions (3.8%) of the Soy1066 WGRS set, and 48 breeding elite lines (7.8%).

Fig. 2 Discrimination clustering plots of samples genotyped with MU-SNAP18-B assay for detection of the *GmSNAP18-b* allele (*rhg1-b*): **a** a set of whole genome re-sequenced GRIN lines; **b** elite breeding lines, and **c**, **d** F₃ populations of either **c** SA18-9022 × LD17-12352 that segregates for *rhg1-b/Rhg1-c*, or **d** JTN-5516 × LD11-2170 that segregates for *rhg1-a/rhg1-b*. The fluorescence of FAM on X-axis was designed to detect the homozygous resistance mutant (MUT) allele (blue). The fluorescence of VIC on Y-axis detects a combination of susceptible wild type (WT) allele and homozygous resistance alleles that are not a desirable (green). Heterozygotes were clustered above MUT haplotype (red). NTC = no template control (grey)



Detection of *GmSNAP15-R* resistance allele at the *cqSCN-006*

The assay MU-SNAP15 (Fig. 6; Supplementary Fig. 6) was developed to separate the FAM[®]-labelled MUT allele named as *GmSNAP15-R* from VIC[®]-labelled WT alleles. Separation angles of all clusters and NTC were near perfect (Fig. 6a, b). The HET cluster was positioned in equal distance between homozygous clusters (Fig. 6c). The allele call rate and assay accuracy were 100% (Supplementary Table 3). This *GmSNAP15-R* created-allele was extremely rare and present in only two accessions (0.2%) of the Soy1066 WGRS set, and three elite breeding lines (0.5%).

Detection of *GmNSF_{RAN07}* resistance allele

The assay MU-NSF-RAN07 (Fig. 7; Supplementary Fig. 7) was designed to detect *GmNSF_{RAN07}* allele consisted of the in-frame insertion variant. The assay determines the FAM[®]-labelled MUT allele *GmNSF_{RAN07}* from VIC[®]-labelled WT alleles. This assay displayed excellent separation of homozygous clusters positioned along their appropriate axis (Fig. 7a, b). Heterozygotes were slightly skewed towards the WT cluster but were easily distinguishable (Fig. 7c). The NTC did not generate any fluorescence.

The allele call rate and assay accuracy were 100% (Supplementary Table 3). This allele was present in 176 accessions (16.5%) of the Soy1066 WGRS set and 591 elite breeding lines (95.5%). Interestingly, PI 468916 (*Glycine soja*) was the only SCN resistant line that amplified WT allele. After the SAC analysis, it was revealed that PI 468916 has one missense mutation at Gm07:36,440,012 not present in other SCN resistant lines. This indicates either an unknown variant at *GmNSF_{RAN07}* may be responsible for the function, or there is a different mode of action in PI 468916.

Detection of *GmSNAP02-ins* and *GmSNAP02-del* alleles

Due to the nature of the mutation, non-standard TaqMan[®] assays were previously designed [24] based on a strategy similar to assay GSM182 that detects the deletion at the *FAD3A* gene [10]. The assay MU-SNAP02^{INS}-WT was developed to amplify a mixture of genotypes without insertion (WT) and HETs. The assay MU-SNAP02^{INS}-MUT amplifies a mixture of genotypes with insertion *GmSNAP02-ins* (MUT) and HETs. Allele Y (green) was automatically assigned by the software to the amplification signal for both assays. These two assays were run with sample Sets 1 through 3 in this study for comparison to the other developed

Fig. 3 Discrimination clustering plots of samples genotyped with MU-SNAP18-C assay for detection of the *GmSNAP18-a* (*rhg1-a*) and *GmSNAP18-b* (*rhg1-b*) alleles: **a** a set of whole genome re-sequenced GRIN lines; **b** elite breeding lines, and **c, d** F_3 populations of either **c** SA18-9022×LD17-12352 that segregates for *rhg1-b/Rhg1-c*, or **d** SA18-13420×U15-322140 that segregates for *rhg1-a/Rhg1-c*. The fluorescence of FAM on X-axis was designed to detect two homozygous resistance mutant alleles (blue): *GmSNAP18-b* as MUT1 cluster, and *GmSNAP18-a* as MUT2 cluster. The fluorescence of VIC on Y-axis detects susceptible wild type (WT) alleles. Position of heterozygotes were marked in red. NTC = no template control (grey). The circles indicate the samples separating MUT1 and MUT2 clusters

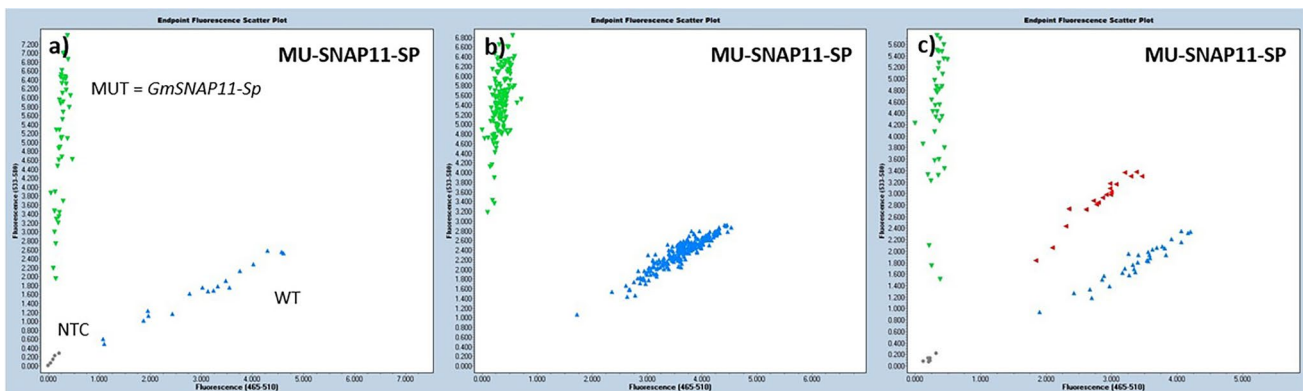
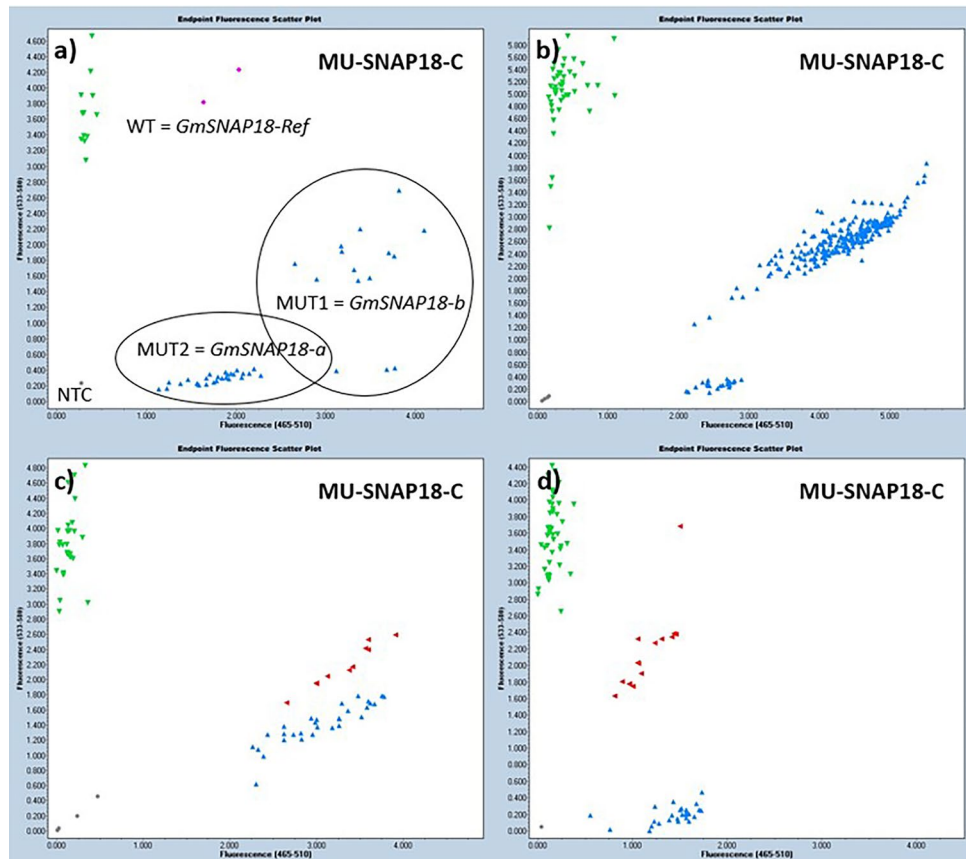


Fig. 4 Discrimination clustering plots of samples genotyped with MU-SNAP11-SP assay for detection of the *GmSNAP11-Sp* (*rhg2*) allele: **a** a set of whole genome re-sequenced GRIN lines; **b** elite breeding lines, and **c** BC_3F_3 population of SA13-1385×SA18-17499. The fluorescence of VIC on Y-axis was designed to detect the

homozygous resistance mutant (MUT) allele *GmSNAP11-Sp* (green). The fluorescence of FAM on X-axis detects a susceptible wild type (WT) alleles (blue). Heterozygotes were clustered within the intermediate (red). NTC = no template control (grey)

assays (Supplementary Fig. 8). Both assays displayed strong amplification and non-ambiguous results. The allele call rate and assay accuracy were 100% (Supplementary Table 4). The *GmSNAP02-ins* allele was present in two accessions (0.2%) of the Soy1066 WGRS set, and none of breeding elite lines (0%).

To separate three alleles at the same variant position, two assays have been previously designed [24] and tested in this research on Set 1 through 3 to validate their performance (Supplementary Fig. 9). The MU-SNAP-02^{DEL}-1 assay (Supplementary Fig. 9a-c) discriminates the VIC[®]-labelled *GmSNAP02-del* allele (MUT cluster)

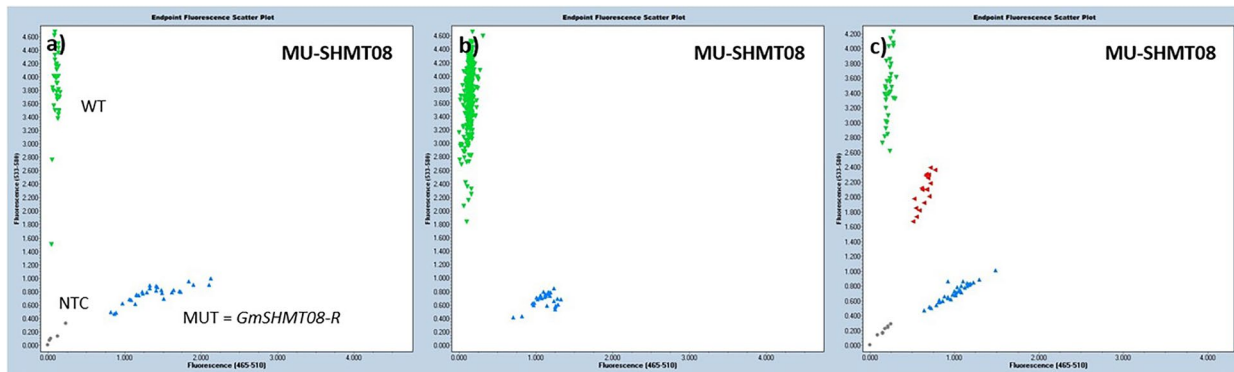


Fig. 5 Discrimination clustering plots of samples genotyped with MU-SHMT08 assay for detection of the *GmSHMT08-R* (*Rhg4*) allele: **a** a set of whole genome re-sequenced GRIN lines; **b** elite breeding lines, and **c** F_3 population of SA17-8882×SA19-12541. The fluorescence of FAM on X-axis detects the homozygous resistance mutant

(MUT) allele *GmSHMT08* (blue). The fluorescence of VIC on Y-axis was designed to detect susceptible wild type (WT) alleles (green). Heterozygotes were clustered within the intermediate (red). NTC=no template control (grey)

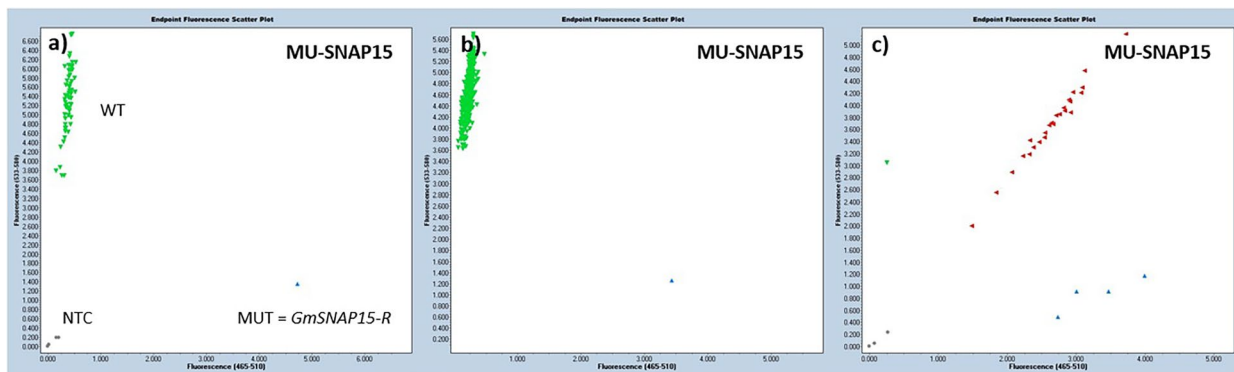


Fig. 6 Discrimination clustering plots of samples genotyped with MU-SNAP15 assay for detection of the *GmSNAP15-R* allele: **a** a set of whole genome re-sequenced GRIN lines; **b** elite breeding lines, and **c** F_1 populations of LD17-10786×U14-910097 and LD20-5738×U14-910097. The fluorescence of FAM on X-axis detects the

homozygous resistance mutant (MUT) allele *GmSNAP15-R* (blue). The fluorescence of VIC on Y-axis was designed to detect susceptible wild type (WT) alleles. Heterozygotes were clustered within the intermediate (red). NTC=no template control (grey)

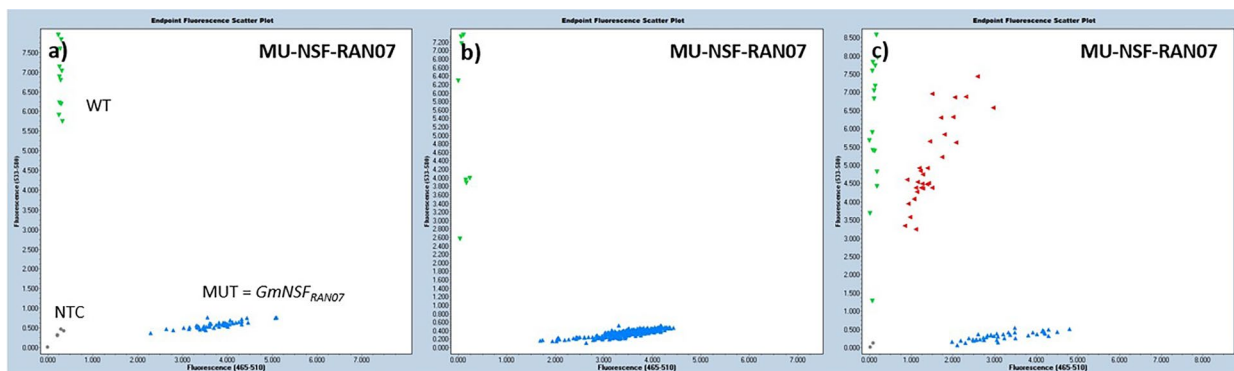


Fig. 7 Discrimination clustering plots of samples genotyped with MU-NSF-RAN07 assay for detection of the *GmNSF_{RAN07}* allele: **a** a set of whole genome re-sequenced GRIN lines; **b** elite breeding lines, and **c** F_3 population of SA18-10037×SA18-350PR. The fluorescence of FAM on X-axis detects the homozygous resistance mutant (MUT)

allele *GmNSF_{RAN07}* (blue). The fluorescence of VIC on Y-axis was designed to detect susceptible wild type (WT) alleles (green). Heterozygotes were clustered within the intermediate (red). NTC=no template control (grey)

from FAM[®]-labelled *GmSNAP02-Alt* allele (WT cluster). For this assay, the remaining genotypes that carry *GmSNAP02-Ref* did not amplify and clustered with NTC, as expected. On the contrary, the MU-SNAP02^{DEL}-2 assay (Supplementary Fig. 9d-f) discriminates the VIC[®]-labelled MUT *GmSNAP02-del* allele (MUT cluster) from ten FAM[®]-labelled *GmSNAP02-Ref* alleles (WT cluster). In contrast, soybean genotypes that carry *GmSNAP02-Alt* allele did not amplify and clustered with NTC, as expected. Both assays had near perfect homozygous cluster to axis separation angles and homozygous cluster to heterozygous cluster separation angles. Depending on the genotyping goal, running only one assay is sufficient in determination of the *GmSNAP02-del* allele, however both assays are needed to distinguish a difference between *GmSNAP02-Ref* and *GmSNAP02-Alt*. PI 407788A did not type a correct allele of WT, and was scored as MUT indicating that this line carries *GmSNAP02-del* (Supplementary Table 4), and therefore, the assay accuracy was 98%. The *GmSNAP02-del* allele was present in seven accessions (0.7%) of the Soy1066 WGRS set, and none of elite breeding lines (0%).

Comparison with currently available assays

Recently, four TaqMan[®] assays have been developed for detection of two alleles of *GmSNAP02* [24]. To our knowledge, no other TaqMan[®] assays are available for high-throughput detection of SCN resistance-causing SNPs or InDels, although, a TaqMan-based copy number assay have been developed [38, 40]. Several KASP[™] and CAPS genotyping assays have been published for detection of resistance at *GmSNAP18*, *GmSNAP11*, and *GmSHMT08*. The comparison of the assays that target the genes' sequence are presented in Table 1. Two sets of KASP[™] assays have been published for detecting the resistance alleles of *GmSNAP18* at the *Rhg1* locus [11, 38]. In both cases, assays GSM 383 (Shi et al. 2015b) and Rhg1-5 [38] were developed to distinguish between *GmSNAP18-a* and *GmSNAP18-b* alleles, however the selection can be made using only *GmSNAP18-a* genotypes. The *GmSNAP18-b* genotypes often cannot be selected using these assays as they cluster with *GmSNAP18-Ref*. Among these two assays, GSM 383 targets the same SNP position as the MU-SNAP18-A TaqMan assay developed in this study. Therefore, GSM 383 and MU-SNAP18-A were developed for selection of *GmSNAP18-a* genotypes and are equally recommended to be used interchangeably depending on the genotyping platform preference. For detection and selection of *GmSNAP18-b* genotypes, MU-SNAP18-B TaqMan assay has been developed in this study and does not have an equivalent KASP[™] assay to be recommended.

KASP[™] assays GSM 381 [11] and Rhg1-5 [38] were developed for separation of the *rhg1* resistant genotypes

from the susceptible genotypes. Similarly, SNAP18-1 and SNAP18-2 assays detect the same clusters, although, they were developed for reniform nematode resistance [39]. In recent years, it has been shown that two known resistant alleles *GmSNAP18-a* and *GmSNAP18-b* underlie different types of SCN resistance that causes unrelated requirements of stacking them with other SCN host genes [15, 17, 24].

Three KASP[™] and one CAPS (Cleaved Amplified Polymorphic Sequences) assays have been developed for detection of *GmSNAP11* resistance at the *Rhg2* locus [20, 31, 39, 41, 42]. The KASP[™] assay GSM151 [42] and CAPS assay GmSNAP11-2565 [41] target the same splice variant position as MU-SNAP11-SP; however the CAPS assay, although proven to be useful in MAS, cannot be utilized in high throughput genotyping due to requirement of restriction endonuclease digestion and running gel electrophoresis steps. Two KASP[™] assays, SNAP11-1 [39] and GmSNAP11-5149 [31], target UTR'3 and a different missense mutation, respectively. Therefore, MU-SNAP11-SP and GSM151 are considered as the best choice of detection of resistance caused by *GmSNAP11*.

Lastly, three KASP[™] assays, GSM 191 (Shi et al. 2015b), Rhg4-3 and Rhg4-5 [38], have been developed for detection of *GmSHMT08* resistance at the *Rhg4* locus. The KASP[™] assay GSM 191 [11], CAPS assay Rhg4-389 [42], and MU-SHMT08 target the same SNP variant position and can be used interchangeably depending on the genotyping platform preference.

Discussion

To correctly identify SCN resistance genes and their alleles and improve the efficiency and cost-effectiveness of molecular breeding techniques, it is necessary to develop accurate molecular marker assays for high-throughput marker-assisted selection methods. This research was done to develop a trait introgression resource for marker-assisted breeding of SCN resistance. TaqMan[®] technology has been selected for its flexibility in assay design criteria and advantage in separating clusters for easy allele determination. This panel of TaqMan[®] assays reflects current knowledge about known SCN resistance-causing genes in soybean genome. This study analyzed available alleles for each target gene and selected the variant position with the highest probability of being a phenotypically causative mutation. These variants included missense/silent mutations, alternative splicing, and various length InDels that could alter the function of the resulting protein. Each assay is detecting the status at one variant position and discriminates one target allele from other existing alleles except MU-NSF-RAN07 that detects the same variant present in four alleles.

Table 1 Summary and comparison of currently available assays for detection of SCN resistance-causing target genes and their relevant alleles

Target gene	Assay name	MUT Allele	MUT Cluster	Position (Wm82. a2.v1)	Type	(WT/MUT) Cause	Reference
<i>GmSNAP18</i>	MU-SNAP18-A	<i>GmSNAP18-a</i>	Allele X	Gm18:1,643,660 Exon 6	TaqMan	C/G D208E	This study
	GSM383	<i>GmSNAP18-a</i>		Gm18:1,643,660 Exon 6	KASP	C/G D208E	[11]
	Rhg1-2	<i>GmSNAP18-a</i>		Gm18:1,643,225 Intron 5	KASP	G/C	[38]
<i>Glyma.18G022500 (Rhg1)</i>	MU-SNAP18-B	<i>GmSNAP18-b</i>	Allele X	Gm18:1,643,643 Exon 6	TaqMan	C/A Q203K	This study
	MU-SNAP18-C	<i>GmSNAP18-a/b</i>	Allele X	Gm18:1,645,409 Exon 9	TaqMan	C/A L288I	This study
	GSM381	<i>GmSNAP18-Ref</i>		Gm18:1,645,409 Exon 9	KASP	C/A L288I	[11]
	Rhg1-5	<i>GmSNAP18-Ref</i>		Gm18:1,644,968 Intron 8	KASP	C/G	[38]
	SNAP18-1	<i>GmSNAP18-Ref</i>		Gm18:1,645,012 Intron 8	KASP	T/G	[39]
	SNAP18-2	<i>GmSNAP18-Ref</i>		Gm18:1,643,107 Intron 5	KASP	C/G	[39]
<i>GmSNAP11 Glyma.11g234500 (Rhg2)</i>	MU-SNAP11-SP	<i>GmSNAP11-Sp</i>	Allele Y	Gm11:32,969,916 Exon 7	TaqMan	C/A Splice	This study
	GSM151	<i>GmSNAP11-Sp</i>		Gm11:32,969,916 Exon 7	KASP	C/A Splice	[20]
	GmSNAP11-2565	<i>GmSNAP11-Sp</i>		Gm11:32,969,916 Exon 7	CAPS	C/A Splice	[41]
	SNAP11-1	<i>GmSNAP11</i>		Gm11:32,968,127 3'UTR	KASP	A/T	[39]
	GmSNAP11-5149	<i>GmSNAP11</i>		Gm11:32,970,174 Exon 6	KASP	C/T A179T	[31]
<i>GmSHMT08 Glyma.08g108900 (Rhg4)</i>	MU-SHMT08	<i>GmSHMT08-R</i>	Allele X	Gm08:8,361,148 Exon 2	TaqMan	C/G P85R&P130R	This study
	GSM191	<i>GmSHMT08-R</i>		Gm08:8,361,148 Exon 2	KASP	C/G P85R&P130R	[11]
	Rhg4-389	<i>GmSHMT08-R</i>		Gm08:8,361,148 Exon 2	CAPS	C/G P85R&P130R	[42]
	Rhg4-3	<i>GmSHMT08</i>		Gm08:8,357,600 Promoter	KASP	A/T	[38]
	Rhg4-5	<i>GmSHMT08</i>		Gm08:8,356,824 Promoter	KASP	G/C	[38]
<i>GmSNAP15 Glyma.15g191200</i>	MU-SNAP15	<i>GmSNAP15-R</i>	Allele X	Gm15:20,631,002 Exon 5	TaqMan	G/T Silent	This study
<i>GmNSF07 Glyma.07g195900</i>	MU-NSF-RAN07	<i>GmNSF_{RAN07}</i>	Allele X	Gm07:36,448,342 Exon 3	TaqMan	C/CAAA F115dup	This study
<i>GmSNAP02 Glyma.02g260400</i>	MU-SNAP02 ^{INS} -WT	<i>GmSNAP02-ins</i>	Negative	Gm02:44,697,705 Exon 8	TaqMan	6 kb insertion	[24]
	MU-SNAP02 ^{INS} -MUT*	<i>GmSNAP02-ins</i>	Allele Y	Gm02:44,697,705 Exon 8	TaqMan	6 kb insertion	[24]
	MU-SNAP-02 ^{DEL} -1**	<i>GmSNAP02-del</i>	Allele Y	Gm02:44,695,753 Exon 1	TaqMan	22 nt deletion	[24]
	MU-SNAP-02 ^{DEL} -2**	<i>GmSNAP02-del</i>	Allele Y	Gm02:44,695,753 Exon 1	TaqMan	22 nt deletion	[24]

Bold values indicate assays developed for this study

There are many factors that can contribute to issues with cluster separation including sample preparation, the instrument, the software, PCR parameters, design of the assay and/or the sample. Ideally, the discrimination plot should show three clusters and the no-template control. The points in each cluster should be grouped closely together and each cluster should be located well away from the other clusters. However, the plots do not always present a three-cluster pattern. In case of MU-SNAP18-B assay, the unexpected pattern is caused by difficult-to-design sequence where the target SNP has been located (Gm18:1,643,643). Although this variant position is bi-allelic and separates *GmSNAP18-b* allele from the other four existing alleles, the additional SNP was present under the sequence where the reverse primer aligns. That non-target SNP (Gm18:1,643,660) is crucial in separation of *GmSNAP18-a* allele from the other existing alleles and is causing the atypical clustering pattern. It is possible to observe additional clusters called angle clusters or a lack of amplification of the sample when there is an additional polymorphism under the primer. The presence of a polymorphism under a primer generally leads to lower PCR efficiency.

Using sequence variations to characterize the alleles works most of the time for breeding on a generation-by-generation basis. However, SCN resistance at *Rhg1* and *Rhg4* loci is also mediated by copy number variation (CNV) [16, 27]. Based on the *rhg1-b* allele present in PI 88788, a set of four genes including *GmSNAP18*, are tandemly repeated nine times [30, 37] and the SCN resistance efficacy of *rhg1-b* alleles scales with copy number [37]. It was also shown that the *rhg1-b* CNV is unstable over multiple generations of breeding [37]. Some inbred cultivars could be heterogeneous for *Rhg1* copy number where the individual plants appear to have diverse copies of the repeat [37]. Extensive CNV exists between resistant soybean accessions, and the sequence diversity also exists within the repeated unit [30, 37]. Remarkable sequence identity does exist between most of the ~31–36 kb *Rhg1* repeat copies [30, 37], however, the *rhg1-b* repeated sequence contains eight or nine *GmSNAP18-b* genes and one *GmSNAP18-Ref* gene. Therefore, there is 9.3 repeats of the PI 88788-type segment that also contains 0.7 repeat of a Williams 82 at the end of the repeated sequence [30, 37]. Moreover, the reduced copy number *rhg1-b* haplotypes, as in cultivar (cv.) ‘Cloud’ (PI 548316) that carries seven copies, also present a partial Williams 82 repeat [30]. This heterogeneity between repeats in high-copy but not low-copy *Rhg1*-containing lines could impact the TaqMan assays to detect *GmSNAP18-b* alleles. Although it has been shown that alleles of *GmSNAP18* highly correlate with copy number variation (CNV) [30, 37], the set of TaqMan assays developed in this study detect structural variations of the target genes. Using MU-SNAP18-B in a

segregating population causes segregating copies to have a strong fluorescent signal that is being clustered by the software near MUT homozygotes. It is unknown how the repeats and CNV of *rhg1* reshuffle in segregating populations. For detection of heterozygotes, it is recommended to use MU-SNAP18-A assay for populations segregating for *rhg1-a/Rhg1-c* and *rhg1-a/rhg1-b*; and MU-SNAP18-C assay for populations segregating for *rhg1-a/Rhg1-c* and *rhg1-b/Rhg1-c*. Separation of heterozygotes using assays MU-SNAP18-B and MU-SNAP18-C in populations segregating for *rhg1-a/rhg1-b* is more difficult; however, the samples display better separation when the *Rhg1-c* control sample like Williams 82 is not included in the assay. Removing *Rhg1-c* control sample from an assay testing for the *rhg1-a/rhg1-b* segregating population would cause the software to create a discrimination plot with improved separation of the heterozygous cluster.

A copy number polymorphism for a gene may or may not appear as an anomaly in the allelic discrimination plot. Data points for samples from homozygous individuals with extra copies of a gene will generally cluster with the homozygous cluster as is the case of MU-SNAP18-A. If an individual is heterozygous with an odd number of copies and the copies have different genotypes, then the data points will most likely fall between the clusters for the heterozygote and the homozygote. For MU-SNAP18-A assay, the shift in positions of heterozygotes in populations segregating for *rhg1-a/Rhg1-c*, and *rhg1-a/rhg1-b*, is likely caused by the presence of CNV. While the MUT cluster represents the *GmSNAP18-a* allele, the WT cluster contains all alleles of *GmSNAP18* including *GmSNAP18-b*. For this reason, in a population segregating for *rhg1-a* and *rhg1-b*, the HET cluster is shifted towards WT. In the case of MU-SNAP18-B, the HET cluster falls directly above the homozygous MUT cluster that interferes with the selection of the correct genotypes. Clustering HET with MUT is also suspected to happen due to segregation of high copy of *rhg1-b* that causes strong fluorescence signal similar to the MUT homozygotes. Since CNV may segregate within the progenies, a gene dosage assay should be performed complimentary to determine which samples carry extra copies of the gene because copy number of *rhg1-b* correlates with efficacy of SCN [30, 37, 40]. Although MU-SNAP18-B assay is not perfect, it can be successfully utilized for the selection of *GmSNAP18-b*. To overcome the limitations of current genotyping methods for selection of homozygotes and heterozygotes of *rhg1-b*, the MU-SNAP18-C assay was developed as a similar approach that was used while developing KASP assays [11, 38].

The position of HET cluster and its equal distance to WT and MUT clusters is significant in determining the correct genotype and avoiding false results in the segregating populations. Discrimination plots of MU-SNAP18-A, MU-SNAP11-SP, and MU-NSF-RAN07 show slight skewness

of HET cluster towards WT cluster, however, these assays separate the desirable MUT alleles effectively, reducing the false-positive scoring to minimum.

TaqMan[®] assays are robust in genotyping multiple variant types, including point mutations, small InDels, and presence/absence variants; but not suitable for InDels larger than 6 bp. All assays that detect resistance-causing alleles of *GmSNAP02* function differently than standard TaqMan[®] assays, as the lack of detection of fluorescence is considered as a part of the results. MU-SNAP02^{INS}-WT and MU-SNAP02^{INS}-MUT work complimentary to detect resistance causing a 6 kb insertion in the *GmSNAP02-ins* allele. When the sample does not have a portion of the gene that contains the target polymorphism, the individual has a null allele and will cluster with the NTC. MU-SNAP02^{INS}-WT amplifies only non-desirable WT alleles and heterozygotes and serves as an amplification control, whereas the desirable MUT allele clusters with NTC. To separate MUT allele from NTC, MU-SNAP02^{INS}-MUT assay is needed. It amplifies only desirable MUT alleles and heterozygotes, whereas the non-desirable WT allele clusters with NTC. For these reasons, these assays behave like a dominant marker. It is recommended to run both assays to distinguish all three correct clusters. Assays MU-SNAP02^{DEL}-1 and MU-SNAP02^{DEL}-2 detect resistance caused by the 22 bp deletion in the *GmSNAP02-del* allele. Most SNP genotyping methods assume that the SNP is biallelic. However, the target position is tri-allelic, and therefore, two assays are needed to distinguish the difference. This study unveiled positions of heterozygous clusters that were not presented in the original publication [24]. MU-SNAP02^{DEL}-1 amplifies non-desirable *GmSNAP02-Alt* allele as WT and desirable *GmSNAP02-del* allele as MUT, whereas the non-desirable *GmSNAP02-Ref* allele clusters with NTC. In contrary, MU-SNAP02^{DEL}-2 amplifies non-desirable *GmSNAP02-Ref* allele as WT and desirable *GmSNAP02-del* allele as MUT, whereas the non-desirable *GmSNAP02-Alt* allele clusters with NTC. The assays were designed to avoid occurrence of outlier samples in the allelic discrimination plot and distinguish the difference between non-amplified allele and NTC.

Many functional polymorphisms occur at low frequencies [43]. The SNP targeted by MU-SNAP15 assay is present at a low minor allele frequency (MAF). Therefore, there is a risk that only one cluster could occur in a population being studied. If the sample size is small, it may not detect rare alleles. Determination of the size of the population is needed to detect the minor allele of interest using the Hardy–Weinberg Equilibrium equation [43]. For this reason, it is important to include the MUT control sample for identification of the correct cluster and for balanced placing of clusters in the discrimination plot by the software.

The discrepancies between WGRS and TaqMan genotyping of two lines, PI 567416 and PI 407788A, set three

assays' accuracies at 98%. Due to the same allele detected by MU-SNAP18-B and MU-SNAP18-C, it was concluded that both assays detected the correct *GmSNAP18-b* allele in PI 567416 (Supplementary Table 2). In a similar case, the same *GmSNAP02-del* allele was detected in PI 407788A using two assays MU-SNAP02^{DEL}-1 and MU-SNAP02^{DEL}-2 (Supplementary Table 4). It is also possible that there are other currently unknown variants may play a role in SCN resistance. These two PIs need further validation in diverse populations. The present assays succeeded in accurately reporting the correct allele associated with known resistance-causing variants including heterozygotes. Three sets of genotyping material were used to address sensitivity and specificity of the assays. If other alleles are reported to play a role in SCN resistance for any of the genes in the future, there would be a need to develop additional assays that target the causative variant.

Soybean breeding programs heavily rely on marker-assisted selection (MAS) to enable the efficient introgression of important traits of interest. Breeding for next generation of SCN-resistant cultivars requires correct understanding of the tradeoffs between different genotyping approaches while making pragmatic and informed decisions regarding selections of SCN gene stacks. Specific gene pyramids with *rhg1-a* or *rhg1-b* have been shown to enhance the efficacy of SCN resistance [17, 24, 44–47]. For example, epistatic effects between *GmSNAP18-a* and *GmSHMT08* [15, 27, 48, 49], *GmSNAP18-a* and *GmSNAP11* [17, 19, 20, 24, 47], and *GmSNAP18-a*, *GmSNAP11*, and *GmSNAP02* [24] have been reported. The TaqMan[®] technology delivers the specificity, sensitivity, and reproducibility that is desired for MAS and is used widely by researchers and breeders for developing and implementing breeder-friendly molecular markers. Development of assays in this research was facilitated by the availability of genome sequence data that are publicly available as genomic variants through SAC. The presently reported panel of SCN TaqMan[®] assays is relatively affordable based on current market standards, easy to run, and it provides an alternative of genotyping platform. Previously developed KASP[™] assays GSM381 and GSM383 for *GmSNAP18* and GSM191 for *GmSHMT08* [11] and GSM151 for *GmSNAP11* [20], target the same genes and their variants as TaqMan assays and are equally recommended as efficient and reliable genotyping method; however, no KASP[™] assays have been reported that target the other genes known to improve SCN resistance. The panel of TaqMan[®] assays developed in this study cover published SCN resistance-causing genes, generate consistent and accurate data with scalable and cost-effective solutions, and can be easily integrated with automated liquid handling systems as a routine genotyping platform for marker deployment and foreground and background

selections in plant breeding. This panel is a tool that can be utilized with minimal additional optimization by plant pathologists, geneticists, breeders, and other researchers.

Supplementary Information The online version contains supplementary material available at <https://doi.org/10.1007/s11033-024-10114-6>.

Author Contribution All authors contributed to the conception and design of the article, interpretation of the relevant literature, and revision of the manuscript. M.U. conceived the study, analyzed alleles, designed and tested the assays, and wrote the manuscript draft. K.B. and A.B. analyzed selected alleles from the raw sequencing reads. A.S. acquired funding and supervised the project. All authors have read and agreed to the published version of the manuscript.

Funding The authors acknowledge financial support of this research from the Missouri Soybean Merchandising Council (16-400-23 and 16-400-24 to A.S. and M.U.), the United Soybean Board (2312-209-0301 and 2412-209-0102 to A.S.; and 2312-209-0601 and 2412-209-0301 to A.B. and A.S.).

Data Availability The datasets generated during the current study are available in the online version of the supplementary material. The dataset of genotyped 619 elite breeding lines of the Northern Soybean Breeding Program of the University of Missouri (Set 2) can be obtained from the corresponding author on reasonable request. Data is provided within the manuscript or supplementary information files.

Declarations

Conflict of interest The authors declare no competing interests.

Ethical Statements Not applicable.

Open Access This article is licensed under a Creative Commons Attribution-NonCommercial-NoDerivatives 4.0 International License, which permits any non-commercial use, sharing, distribution and reproduction in any medium or format, as long as you give appropriate credit to the original author(s) and the source, provide a link to the Creative Commons licence, and indicate if you modified the licensed material. You do not have permission under this licence to share adapted material derived from this article or parts of it. The images or other third party material in this article are included in the article's Creative Commons licence, unless indicated otherwise in a credit line to the material. If material is not included in the article's Creative Commons licence and your intended use is not permitted by statutory regulation or exceeds the permitted use, you will need to obtain permission directly from the copyright holder. To view a copy of this licence, visit <http://creativecommons.org/licenses/by-nc-nd/4.0/>.

References

- Jiang GL, Rajcan I, Zhang YM, Han T, Mian R (2023) Editorial: soybean molecular breeding and genetics. *Front Plant Sci* 14:1157632. <https://doi.org/10.3389/fpls.2023.1157632>
- Gladman N, Goodwin S, Chougule K, Richard McCombie W, Ware D (2023) Era of gapless plant genomes: innovations in sequencing and mapping technologies revolutionize genomics and breeding. *Curr Opin Biotechnol* 79:102886. <https://doi.org/10.1016/j.copbio.2022.102886>
- Thomas WJW, Zhang Y, Amas JC, Cantila AY, Zandberg JD, Harvie SL, Batley J (2023) Innovative advances in plant genotyping. *Methods Mol Biol* 2638:451–465. https://doi.org/10.1007/978-1-0716-3024-2_32
- Song QJ, Yan L, Quigley C, Fickus E, Wei H, Chen LF, Dong FM, Araya S, Liu JL, Hyten D, Pantalone V, Nelson RL (2020) Soybean BARCSoySNP6K: an assay for soybean genetics and breeding research. *Plant J* 104:800–811. <https://doi.org/10.1111/tbj.14960>
- Yang Q, Zhang J, Shi X, Chen L, Qin J, Zhang M, Yang C, Song Q, Yan L (2023) Development of SNP marker panels for genotyping by target sequencing (GBTS) and its application in soybean. *Mol Breed* 43:26. <https://doi.org/10.1007/s11032-023-01372-6>
- Schleinitz D, Distefano JK, Kovacs P (2011) Targeted SNP genotyping using the TaqMan^(R) assay. *Methods Mol Biol* 700:77–87. https://doi.org/10.1007/978-1-61737-954-3_6
- He C, Holme J, Anthony J (2014) SNP genotyping: the KASP assay. *Methods Mol Biol* 1145:75–86. https://doi.org/10.1007/978-1-4939-0446-4_7
- Andersen CB, Holst-Jensen A, Berdal KG, Thorstensen T, Tengs T (2006) Equal performance of TaqMan, MGB, molecular beacon, and SYBR green-based detection assays in detection and quantification of roundup ready soybean. *J Agric Food Chem* 54:9658–9663. <https://doi.org/10.1021/jf061987c>
- Heissl A, Arbeitshuber B, Tiemann-Boege I (2017) High-Throughput genotyping with TaqMan allelic discrimination and allele-specific genotyping assays. *Methods Mol Biol* 1492:29–57. https://doi.org/10.1007/978-1-4939-6442-0_3
- Pham A-T, Bilyeu K, Chen P, Boerma HR, Li Z (2014) Characterization of the *fan1* locus in soybean line A5 and development of molecular assays for high-throughput genotyping of FAD3 genes. *Mol Breed* 33:895–907. <https://doi.org/10.1007/s11032-013-0003-1>
- Shi Z, Liu S, Noe J, Arelli P, Meksem K, Li Z (2015) SNP identification and marker assay development for high-throughput selection of soybean cyst nematode resistance. *BMC Genomics* 16:314–325. <https://doi.org/10.1186/s12864-015-1531-3>
- Bandara AY, Weerasooriya DK, Bradley CA, Allen TW, Esker PD (2020) Dissecting the economic impact of soybean diseases in the United States over two decades. *PLoS ONE* 15:1–28. <https://doi.org/10.1371/journal.pone.0231141>
- McCarville MT, Daum J, Xing L, Moser H (2023) Soybean cyst nematode management is improved by combining native and transgenic resistance. *Plant Dis* 107:2792–2798. <https://doi.org/10.1094/PDIS-10-22-2515-RE>
- Bent A (2022) Exploring soybean resistance to soybean cyst nematode. *Annu Rev Phytopathol* 60:379–409. <https://doi.org/10.1146/annurev-phyto-020620-120823>
- Liu S, Kandath PK, Lakhssassi N, Kang J, Colantonio V, Heinz R, Yeckel G, Zhou Z, Bekal S, Dapprich J, Rotter B, Cianzio S, Mitchum MG, Meksem K (2017) The soybean GmSNAP18 gene underlies two types of resistance to soybean cyst nematode. *Nat Commun* 8:14822. <https://doi.org/10.1038/ncomms14822>
- Cook DE, Lee TG, Guo XL, Melito S, Wang K, Bayless AM, Wang JP, Hughes TJ, Willis DK, Clemente TE, Diers BW, Jiang JM, Hudson ME, Bent AF (2012) Copy number variation of multiple genes at Rhg1 mediates nematode resistance in soybean. *Science* 338:1206–1209. <https://doi.org/10.1126/science.1228746>
- Basnet P, Meinhardt CG, Usovsky M, Gillman JD, Joshi T, Song Q, Diers B, Mitchum MG, Scaboo AM (2022) Epistatic interaction between Rhg1-a and Rhg2 in PI 90763 confers resistance to virulent soybean cyst nematode populations. *Theor Appl Genet* 135:2025–2039. <https://doi.org/10.1007/s00122-022-04091-2>

18. Bayless AM, Zapotocny RW, Grunwald DJ, Amundson KK, Diers BW, Bent AF (2018) An atypical N-ethylmaleimide sensitive factor enables the viability of nematode-resistant Rhg1 soybeans. *P Natl Acad Sci USA* 115:E4512–E4521. <https://doi.org/10.1073/pnas.1717070115>
19. Suzuki C, Taguchi-Shiobara F, Ikeda C, Iwahashi M, Matsui T, Yamashita Y, Ogura R (2020) Mapping soybean rhg2 locus, which confers resistance to soybean cyst nematode race 1 in combination with rhg1 and Rhg4 derived from PI 84751. *Breeding Sci* 70:474–480. <https://doi.org/10.1270/jsbbs.20035>
20. Shaibu AS, Zhang SR, Ma JK, Feng Y, Huai YY, Qi J, Li J, Abdelghany AM, Azam M, Htway HTP, Sun JM, Li B (2022) The GmSNAP11 contributes to resistance to soybean cyst nematode race 4 in glycine max. *Front Plant Sci* 13:939763. <https://doi.org/10.3389/fpls.2022.939763>
21. Lakhssassi N, Liu SM, Bekal S, Zhou Z, Colantonio V, Lambert K, Barakat A, Meksem K (2017) Characterization of the Soluble NSF attachment protein gene family identifies two members involved in additive resistance to a plant pathogen. *Sci Rep-Uk* 7:1–11. <https://doi.org/10.1038/srep45226>
22. Liu SM, Kandoth PK, Warren SD, Yeckel G, Heinz R, Alden J, Yang CL, Jamai A, El-Mellouki T, Juvalé PS, Hill J, Baum TJ, Cianzio S, Whitham SA, Korkin D, Mitchum MG, Meksem K (2012) A soybean cyst nematode resistance gene points to a new mechanism of plant resistance to pathogens. *Nature* 492:256–+. <https://doi.org/10.1038/nature11651>
23. Butler KJ, Fliege C, Zapotocny R, Diers B, Hudson M, Bent AF (2021) Soybean cyst nematode resistance quantitative trait locus cqSCN-006 alters the expression of a gamma-SNAP protein. *Mol Plant Microbe Interact* 34:1433–1445. <https://doi.org/10.1094/MPMI-07-21-0163-R>
24. Usovsky M, Gamage VA, Meinhardt CG, Dietz N, Triller M, Basnet P, Gillman JD, Bilyeu KD, Song Q, Dhital B, Nguyen A, Mitchum MG, Scaboo AM (2023) Loss-of-function of an alpha-SNAP gene confers resistance to soybean cyst nematode. *Nat Commun* 14:7629. <https://doi.org/10.1038/s41467-023-43295-y>
25. Ayalew H, Tsang PW, Chu C, Wang J, Liu S, Chen C, Ma XF (2019) Comparison of TaqMan, KASP and rhAmp SNP genotyping platforms in hexaploid wheat. *PLoS ONE* 14:e0217222. <https://doi.org/10.1371/journal.pone.0217222>
26. Chan YO, Dietz N, Zeng S, Wang JX, Flint-Garcia S, Salazar-Vidal MN, Skrabisova M, Bilyeu K, Joshi T (2023) The allele catalog tool: a web-based interactive tool for allele discovery and analysis. *BMC Genomics* 24(1):107. <https://doi.org/10.1186/s12864-023-09161-3>
27. Patil GB, Lakhssassi N, Wan JR, Song L, Zhou Z, Klepadlo M, Vuong TD, Stec AO, Kahil SS, Colantonio V, Valliyodan B, Rice JH, Piya S, Hewezi T, Stupar RM, Meksem K, Nguyen HT (2019) Whole-genome re-sequencing reveals the impact of the interaction of copy number variants of the rhg1 and Rhg4 genes on broad-based resistance to soybean cyst nematode. *Plant Biotechnol J* 17:1595–1611. <https://doi.org/10.1111/pbi.13086>
28. King Z, Serrano J, Boerma HR, Li ZL (2014) Non-toxic and efficient DNA extractions for soybean leaf and seed chips for high-throughput and large-scale genotyping. *Biotechnol Lett* 36:1875–1879. <https://doi.org/10.1007/s10529-014-1548-8>
29. Matsye PD, Lawrence GW, Youssef RM, Kim KH, Lawrence KS, Matthews BF, Klink VP (2012) The expression of a naturally occurring, truncated allele of an alpha-SNAP gene suppresses plant parasitic nematode infection. *Plant Mol Biol* 80:131–155. <https://doi.org/10.1007/s11103-012-9932-z>
30. Cook DE, Bayless AM, Wang K, Guo XL, Song QJ, Jiang JM, Bent AF (2014) Distinct copy number, coding sequence, and locus methylation patterns underlie rhg1-mediated soybean resistance to soybean cyst nematode. *Plant Physiol* 165:630–647. <https://doi.org/10.1104/pp.114.235952>
31. Tian Y, Liu B, Shi X, Reif JC, Guan R, Li Y-h, Qiu L-j (2019) Deep genotyping of the gene GmSNAP facilitates pyramiding resistance to cyst nematode in soybean. *Crop J* 7:677–684. <https://doi.org/10.1016/j.cj.2019.04.003>
32. Lejeune F (2022) Nonsense-mediated mRNA Decay, a finely regulated mechanism. *Biomedicines* 10. <https://doi.org/10.3390/biomedicines10010141>
33. Korasick DA, Kandoth PK, Tanner JJ, Mitchum MG, Beamer LJ (2020) Impaired folate binding of serine hydroxymethyltransferase 8 from soybean underlies resistance to the soybean cyst nematode. *J Biol Chem* 295:3708–3718. <https://doi.org/10.1074/jbc.RA119.012256>
34. Korasick DA, Owuocha LF, Kandoth PK, Tanner JJ, Mitchum MG, Beamer LJ (2024) Structural and functional analysis of two SHMT8 variants associated with soybean cyst nematode resistance. *FEBS J* 291:323–337. <https://doi.org/10.1111/febs.16971>
35. Bayless AM, Smith JM, Song JQ, McMinn PH, Teillet A, August BK, Bent AF (2016) Disease resistance through impairment of alpha-SNAP-NSF interaction and vesicular trafficking by soybean Rhg1. *P Natl Acad Sci USA* 113:E7375–E7382. <https://doi.org/10.1073/pnas.1610150113>
36. Broccanello C, Chiodi C, Funk A, JM, Panella L, Stevanato P (2018) Comparison of three PCR-based assays for SNP genotyping in plants. *Plant Methods* 14:28. <https://doi.org/10.1186/s13007-018-0295-6>
37. Lee TG, Kumar I, Diers BW, Hudson ME (2015) Evolution and selection of Rhg1, a copy-number variant nematode-resistance locus. *Mol Ecol* 24:1774–1791. <https://doi.org/10.1111/tbj.13240>
38. Kadam S, Vuong TD, Qiu D, Meinhardt CG, Song L, Deshmukh R, Patil G, Wan JR, Valliyodan B, Scaboo AM, Shannon JG, Nguyen HT (2016) Genomic-assisted phylogenetic analysis and marker development for next generation soybean cyst nematode resistance breeding. *Plant Sci* 242:342–350. <https://doi.org/10.1016/j.plantsci.2015.08.015>
39. Usovsky M, Lakhssassi N, Patil GB, Vuong TD, Piya S, Hewezi T, Robbins RT, Stupar RM, Meksem K, Nguyen HT (2021) Dissecting nematode resistance regions in soybean revealed pleiotropic effect of soybean cyst and reniform nematode resistance genes. *Plant Genome* 14:e20083. <https://doi.org/10.1002/tpg2.20083>
40. Lee TG, Diers BW, Hudson ME (2016) An efficient method for measuring copy number variation applied to improvement of nematode resistance in soybean. *Plant J* 88:143–153. <https://doi.org/10.1111/tbj.13240>
41. Tian Y, Yang L, Li Y, Qiu L (2018) Development and utilization of KASP marker for SCN3-11 locus resistant to soybean cyst nematode. *Acta Agron Sin* 44:1600–1611. <https://doi.org/10.1016/j.cj.2019.04.003>
42. Shi X, Li Y, Yu B, Guo Y, Wang J, Qiu L (2015) Development and utilization of CAPS/dCAPS markers based on the SNPs lying in soybean cyst nematode resistant genes Rhg4. *Acta Agron Sin* 41:1463–1471. <https://doi.org/10.5555/20153389406>
43. Rohlfs RV, Weir BS (2008) Distributions of Hardy-Weinberg equilibrium test statistics. *Genetics* 180:1609–1616. <https://doi.org/10.1534/genetics.108.088005>
44. Meinhardt C, Howland A, Ellersieck M, Scaboo A, Diers B, Mitchum MG (2021) Resistance gene pyramiding and rotation to combat widespread soybean cyst nematode virulence. *Plant Dis* 105:3238–3243. <https://doi.org/10.1094/Pdis-12-20-2556-Re>
45. Brzostowski LF, Diers BW (2017) Pyramiding of alleles from multiple sources increases the resistance of soybean to highly virulent soybean cyst nematode isolates. *Crop Sci* 57:2932–2941. <https://doi.org/10.2135/cropsci2016.12.1007>

46. Kim M, Hyten DL, Niblack TL, Diers BW (2011) Stacking resistance alleles from wild and domestic soybean sources improves soybean cyst nematode resistance. *Crop Sci* 51:934–943. <https://doi.org/10.2135/cropsci2010.08.0459>
47. St-Amour VT, Mimee B, Torkamaneh D, Jean M, Belzile F, O'Donoghue LS (2020) Characterizing resistance to soybean cyst nematode in PI 494182, an early maturing soybean accession. *Crop Sci* 60:2053–2069. <https://doi.org/10.1002/csc2.20162>
48. Wu XL, Blake S, Sleper DA, Shannon JG, Cregan P, Nguyen HT (2009) QTL, additive and epistatic effects for SCN resistance in PI 437654. *Theor Appl Genet* 118:1093–1105. <https://doi.org/10.1007/s00122-009-0965-x>
49. Brucker E, Carlson S, Wright E, Niblack T, Diers B (2005) Rhg1 alleles from soybean PI 437654 and PI 88788 respond differentially to isolates of *Heterodera glycines* in the greenhouse. *Theor Appl Genet* 111:44–49. <https://doi.org/10.1007/s00122-005-1970-3>

Publisher's Note Springer Nature remains neutral with regard to jurisdictional claims in published maps and institutional affiliations.